Specific Features of the Spectral Properties of a Cholesteric Liquid Crystal with a Resonance Defective Nanocomposite Layer

S. Ya. Vetrov[a, b], M. V. Pyatnov[a], *, and I. V. Timofeev[a, b]

[a] *Siberian Federal University, Svobodnyi pr. 79, Krasnoyarsk, 660041 Russia*
* e-mail: MaksPyatnov@yandex.ru
[b] *Kirensky Institute of Physics, Siberian Branch of the Russian Academy of Sciences,
Akademgorodok 50–38, Krasnoyarsk, 660036 Russia*
Received January 21, 2013

Abstract—This paper reports on studying the spectral properties of a cholesteric liquid crystal with a defective layer of a nanocomposite consisting of metallic nanoballs dispersed in a transparent matrix and characterized by an effective resonance dielectric permittivity. The transmission, reflection, and absorption spectra of waves of both circular polarizations have been calculated, and the spectral splitting of the defective mode when its frequency coincides with the resonance frequency of the nanocomposite has been studied. An essential dependence of the splitting on the nanoball concentration in the defect has been established. It has been shown that, depending on the position of the resonance frequency with respect to the boundaries of the cholesteric band gap, an additional passband appears in the transmission spectrum, which corresponds to waves of the diffracting circular polarization, or an additional band gap for waves of both circular polarizations, which are substantially modified with variations of both the incidence angle of light and the cholesteric helix pitch.

1. INTRODUCTION

Materials whose dielectric permittivity periodically varies in one, two, or three dimensions in the spatial scale comparable with the wavelength of light are termed photonic crystals (PCs) or photonic crystal structures. They arouse much interest as new optical materials with unique properties [1–4]. Due to the spatial periodicity, the spectrum of electromagnetic waves in PCs has a band character just as a spatially periodic potential leads to a band character of the electron spectrum. In a photonic crystal with a defect in the lattice, i.e., with distorted periodicity, passbands appear in photonic band gaps, whose position and transmittivity can be controlled by varying geometric and structural parameters [4]. In this case, light is localized near the defect, which leads to an increase in the intensity of the light wave inside the defective layer. On the basis of PC materials with defects, new types of waveguides [5] and high-Q nanocavities [6, 7] were developed and methods for increasing the intensity of nonlinear optical processes were proposed [8, 9].

A special class of one-dimensional photonic crystals is formed by cholesteric liquid crystals (CLCs), which have unique properties: a wide passband, strong nonlinearity, and high sensitivity to external fields [10]. By varying temperature and pressure and by applying electromagnetic fields and mechanical stresses, one can substantially vary the cholesteric helix pitch. A qualitative difference of CLCs from

other kinds of PCs is that their diffraction reflectivity is selective to polarization. CLCs have photonic band gaps for light propagating along the CLC helix axis when its circular polarization coincides with the direction of rotation of the cholesteric helix. When the cholesteric reflects light with such polarization, the sign of polarization remains invariable. Light waves with the opposite circular polarizations do not experience diffraction reflection and pass through the cholesteric medium almost unchanged. Introduction of various types of defects into an ideal CLC structure leads to the emergence of narrow passbands in the band gaps, which correspond to localized defective modes [11–15]. Just as defective modes in scalar periodic layered media, such modes can be used for the development of narrow-band filters and for the low-threshold laser generation. Defective modes of CLCs as materials with photonic band gaps were studied in [11] for the first time by numerical analysis. One of the revealed optical effects connected with a defect in the form of a thin isotropic dielectric layer inserted between cholesteric layers is the induction of defective modes in the CLC band gaps for both circular polarizations of normally incident light. An analytic approach to the theory of optical defective modes in CLCs with an isotropic defective layer was developed in [16] in the framework of a model making it possible to eliminate the polarization mixing and to obtain the equation for light of only the diffracting polarization.
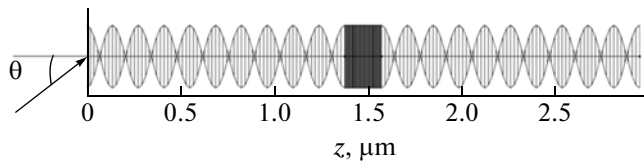
Fig. 1. Schematic representation of the cholesteric structure with a defect.

Fig. 2. Imaginary ε''_{mix} (dashed line) and real ε'_{mix} (solid line) parts of the effective dielectric permittivity ε_{mix} of a nanocomposite vs. the wavelength. The filling factors are $f =$ (a) 0.02 and (b) 0.10.

New possibilities for the control of light appear in one-dimensional photonic crystals with nanostructured metal–dielectric defective layers [17, 18]. A resonance of the effective dielectric permittivity was predicted in a nanocomposite consisting of metallic nanoparticles dispersed in a transparent matrix [19, 20]. In this case, the optical characteristics of the initial materials have no resonance singularities. The position of the resonance, which lies in the visible light band, depends on the dielectric permittivity of the initial materials and the concentration and shape of nanoparticles. In the present work, we study the specific features of CLCs with a defective layer of a nanocomposite consisting of silver nanoballs dispersed in a transparent matrix and characterized by the resonance dielectric permittivity.

2. THE MODEL UNDER STUDY

The considered structure consists of two identical layers of an ideal dexiotropic CLC, separated by a defective nanocomposite layer (Fig. 1). The length of the cholesteric structure is $20P$, where $P = 275$ nm is the pitch of the crystal helix, and the thickness of the defective layer is $d = 5P/7$. The medium outside the cholesteric is isotropic and has the refractive index $n = (n_0 + n_e)/2$, where $n_0 = 1.4$ and $n_e = 1.6$ are the ordinary and extraordinary refractive indices of the CLC, respectively. With such an external medium, the Fresnel reflection from the cholesteric surface and the interference stripes from the boundary surfaces are very weak.

The dielectric permittivity ε_{mix} of the nanocomposite layer is determined by the Maxwell–Garnett formula, which is widely used in consideration of matrix media when isolated inclusions with a small volume content are dispersed in the material of the matrix [19–21]:

$$\varepsilon_{mix} = \varepsilon_d \left[\frac{f}{(1-f)/3 + \varepsilon_d/(\varepsilon_m - \varepsilon_d)} + 1 \right]. \quad (1)$$

Here, f is the filling factor, i.e., the fraction of nanoparticles in the matrix; ε_d and $\varepsilon_m(\omega))$, respectively, are the dielectric permittivities of the matrix and the metal from which nanoparticles are fabricated; and ω is the radiation frequency. The nanoparticle size is significantly smaller than the wavelength and the depth of penetration to the material. The dielectric permittivity
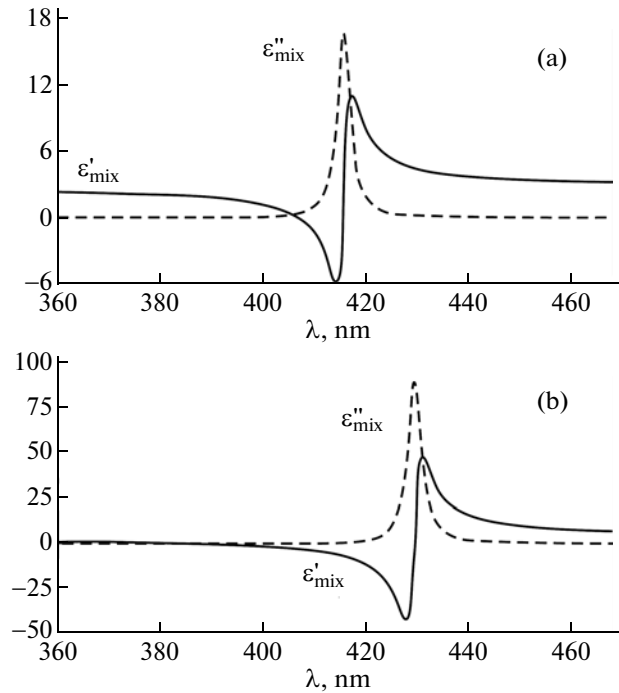
of the metal from which nanoparticles are fabricated can be found using the Drude approximation

$$\varepsilon_m(\omega) = \varepsilon_0 - \frac{\omega}{\omega(\omega + i\gamma)}, \quad (2)$$

where ε_0 is a constant taking into account the contribution of interband transitions, ω_p is the plasma frequency, and γ is the reciprocal electron relaxation time. For silver nanoballs dispersed in transparent optical glass, $\varepsilon_0 = 5$, $\omega_p = 9$ eV, $\gamma = 0.02$ eV, and $\varepsilon_d = 2.56$.

Neglecting the small factor γ^2, we find the position of the resonance frequency, which depends on the characteristics of the initial materials and the dispersed phase concentration f:

$$\omega_0 = \omega_p \sqrt{\frac{1-f}{3\varepsilon_d + (1-f)(\varepsilon_0 - \varepsilon_d)}} \quad (3)$$

Figure 2 shows the dispersion dependence of the dielectric permittivity of the nanocomposite for two values of the filling factor: $f = 0.02$ and 0.10.

It is evident from Fig. 2 that, with an increase in the nanoball concentration, the frequency ω_0 corresponding to the resonance in the defective layer is displaced to the longer-wavelength spectral region. In this case, the width of the resonance curve measured at the half
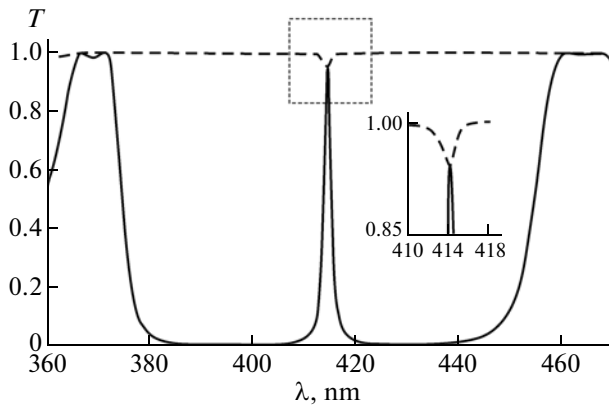
Fig. 3. Transmission spectrum for waves with the right-handed (solid line) and left-handed (dashed line) circular polarizations, $\theta = 0°$. The filling factor is $f = 0$. The inset shows the magnified small peak at 414 nm.

power, ε''_{mix}, varies insignificantly, the curve of ε'_{mix} is substantially modified, and the range of frequencies at which the nanocomposite is similar to metal for $\varepsilon'_{mix} < 0$ is extended.

3. NUMERICAL RESULTS

The numerical analysis of the spectral properties and field distributions in a sample was performed by the method of the Berreman transfer matrix [22], which makes possible a quantitative study of light propagation in CLCs with a defect in the structure. The equation describing the propagation of light with a frequency ω along the z axis reads

$$\frac{d\Psi}{dz} = \frac{i\omega}{c}\Delta(z)\Psi(z), \qquad (4)$$

where $\Psi(z) = (E_x, H_y, E_y, -H_x)^T$ and $\Delta(z)$ is the Berreman transfer matrix, which depends on the dielectric function and the incident wave vector.

Figure 3 shows the seed ($f = 0$) transmission spectrum on the normal incidence of light onto a cholesteric with a defect of the structure in the form of a dielectric plate. It is readily seen from the figure that, like in [11], the photonic band gap has peaks corresponding to defective modes of the CLC, which are induced for both circular polarizations of normally incident light. In addition, the defective modes have the same wavelength and the same transmittivity.

If the filling factor is nonzero and the resonance frequency ω_0 of the nanocomposite coincides with the defective mode frequency, the defective mode frequency is split by analogy with the splitting of the frequencies of two coupled oscillators. The manifestation of the splitting in the transmission, reflection, and absorption spectra is illustrated by Fig. 4. It is evident from Fig. 4a that, as a result of splitting, the defective
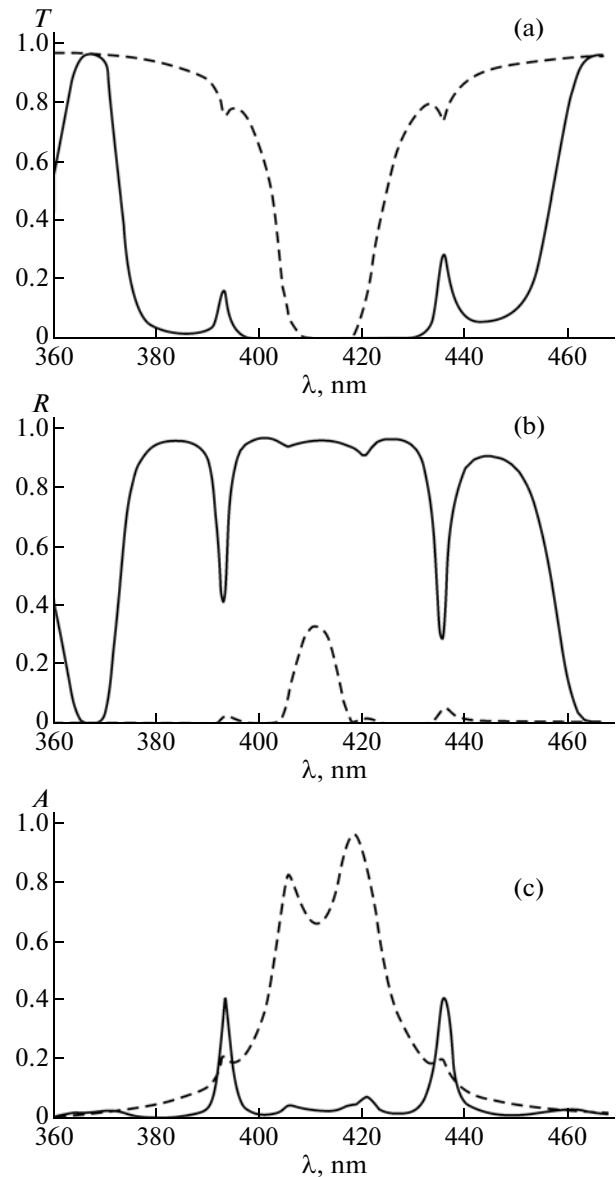

Fig. 4. (a) Transmission (T), (b) reflection (R), and (c) absorption (A) spectra for waves with the right-handed (solid line) and left-handed (dashed line) circular polarizations, $\theta = 0°$. The filling factor is $f = 0.02$.

modes for the right- and left-handed circular polarizations have the same wavelength but different transmittivities at the center of the peak. The computations show that, as like as in a scalar one-dimensional PC with a defective nanocomposite layer [17], the splitting increases with the volume fraction of nanoballs in the composite. For the reflection and absorption spectra (Figs. 4b, 4c), a strong dependence of the reflection and absorption coefficients on the direction of the circular polarization of incident light is typical. The emergence of two defective modes in the spectral range forbidden for both polarizations after the splitting (Fig. 4a) is connected, primarily, with the sub-
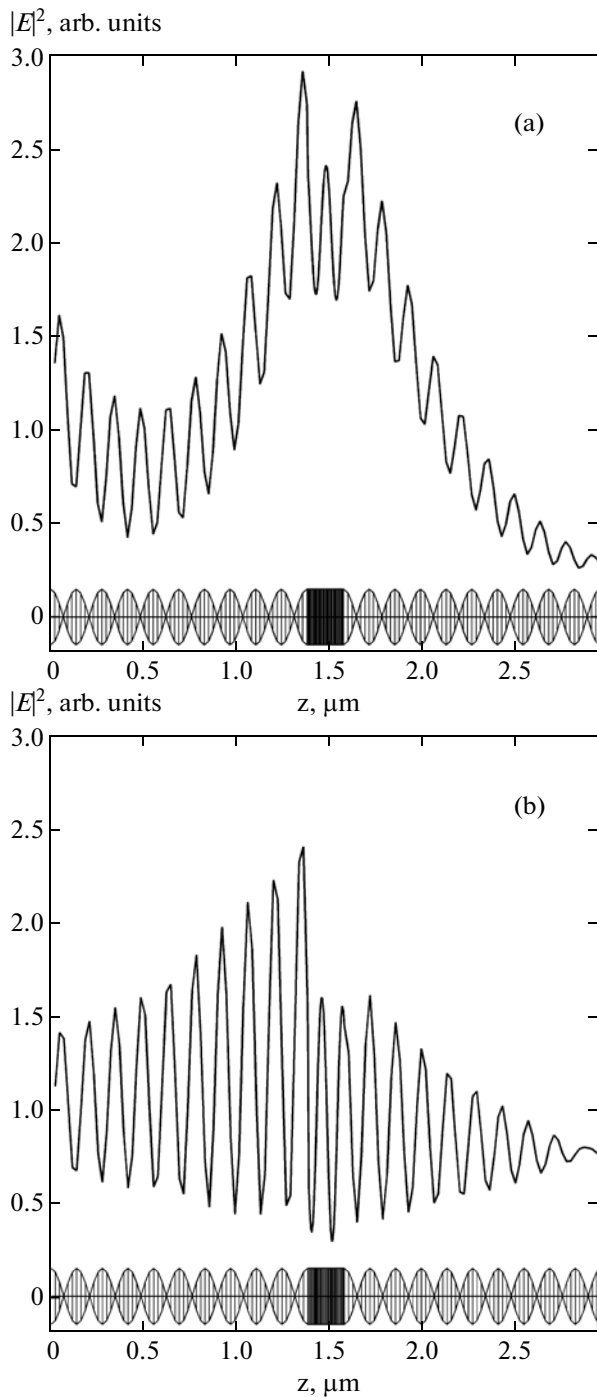
Fig. 5. Distribution of the squared modulus of the electric field for $\lambda = 435.8$ nm (Fig. 4a) and $f = 0.02$ for defective modes with $T = $ (a) 0.30 and (b) 0.76.

Fig. 6. Transmission spectra for the angles of incidence $\theta = $ (a) 26° and (b) 30° for light with the right-handed (solid line) and left-handed (dashed line) circular polarizations. The filling factor is $f = 0.01$.

The field localization manifests itself most distinctly in a region comparable with the wavelength for the mode corresponding to the right-handed diffracting polarization.

New peculiarities in the transmission spectrum appear with variation in the incidence angle of light, θ. With an increase in θ, the band gap of the CLC is displaced, according to the Bragg condition, to the short-wavelength region. In this case, the long-wavelength edge of the photonic band gap shifts to the resonance frequency ω_0 of the defective layer. At $\theta = 26°$ (Fig. 6a), the short-wavelength peak in the photonic band gap, corresponding to the defective mode, disappears and the long-wavelength peak of the defective modes corresponding to the right- and left-handed circular polarizations remains. It should be noted that, for this value of the incidence angle, the resonance frequency ω_0 is found near the long-wavelength boundary of the photonic band gap. Mixing the resonance frequency with photonic modes leads to expansion of the band gap, i.e., an additional passband, corresponding to the diffracting polarization, is split from the long-wavelength edge of the band gap and a rejection band appears in the vicinity of ω_0 for waves of both polarizations, which is caused mainly by the absorption of the field in the nanocomposite layer. With a fur-

stantial reflection and absorption of waves of the right- and left-handed circular polarizations, respectively, (Figs. 4b, 4c).

Figure 5 shows the spatial electric field distribution in defective modes with the wavelength $\lambda = 435.8$ nm (Fig. 4a).
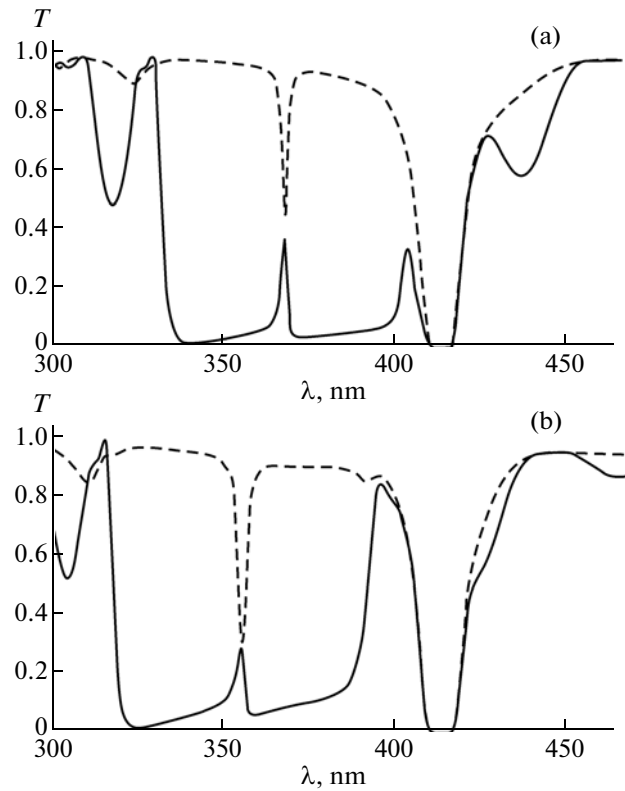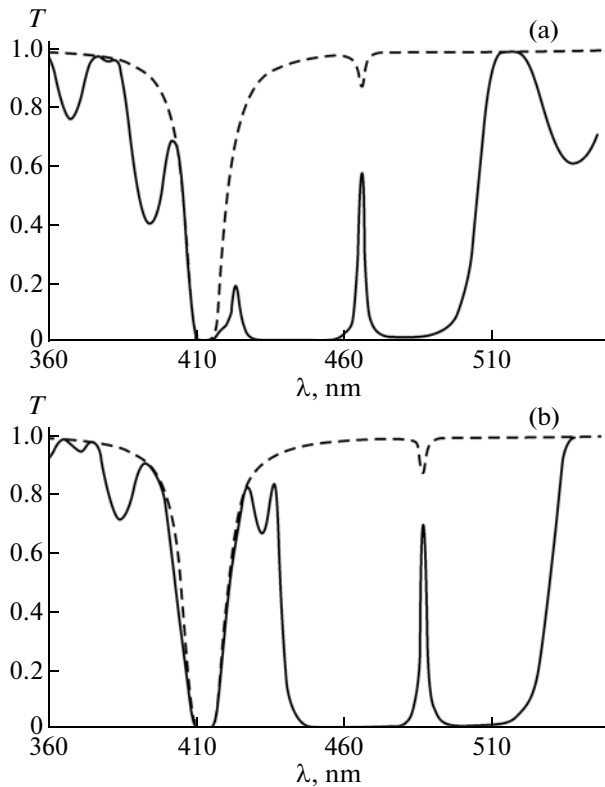
Fig. 7. Transmission spectra for helix pitches $P =$ (a) 305 and (b) 320 nm for waves with the right-handed (solid line) and left-handed (dashed line) circular polarizations. The filling factor is $f = 0.01$.

ther increase in the incidence angle θ, the resonance frequency ω_0 is found in the continuous rejection spectrum. The resonance situations taking place in this case leads to the emergence of an additional band gap (Fig. 6b).

Similar effects can be realized in a different way, by varying the cholesteric helix pitch. Indeed, with an increase in the helix pitch, e.g., due to variation in temperature, the band gap shifts to the long-wave-length region. In this case, mixing the resonance mode with photonic modes leads to splitting the photonic band gap (Fig. 7a) and emergence of an additional rejection band in the continuous spectrum (Fig. 7b).

4. CONCLUSIONS

The spectral properties of a cholesteric liquid crystal with a structural resonantly absorbing defective layer of a nanocomposite consisting of silver nanoballs dispersed in a transparent matrix have been studied. A number of important features in the spectral properties of CLCs with a defect in the structure, which are caused primarily by the resonant character of the effective dielectric permittivity of the nanocomposite and its essential dependence on the filling factor f, have been revealed.

It has been studied how the splitting of frequencies of the defective modes induced for both circular polarizations of incident radiation manifests itself in the transmission, reflection, and absorption spectra. As a result of the splitting of frequencies, a band gap appears in the transmission spectrum. The value of the splitting increases with increasing volume fraction of nanoballs in the defective layer and can reach 50 nm.

It has been shown that the transmission spectrum of a defective CLC can be efficiently controlled by varying the angle of the incidence of light onto the cholesteric or by varying the helix pitch by the action of external fields. There are values of the incidence angle or the helix pitch at which the resonance frequency of the nanocomposite is found near the boundaries of the band gap of the CLC structure, which leads to the emergence of an additional pass-band for waves of the diffracting polarization or an additional rejection band for waves of both circular polarizations.

REFERENCES

1. J. D. Joannopoulos, S. G. Johnson, J. N. Winn, and R. D. Meade, *Photonic Crystals: Molding the Flow of Light*, 2nd ed. (Princeton University Press, Princeton, New Jersey, 2008), p. 286.
2. K. Sakoda, *Optical Properties of Photonic Cristals* (Springer-Verlag, Berlin, 2004), p. 253.
3. K. Busch, S. Lölkes, R. B. Wehrspohn, and H. Föll, *Photonics Cristals: Advances in Design, Fabrication and Characterization* (Wiley, Weinheim, 2004), p. 354.
4. V. F. Shabanov, S. Ya. Vetrov, and A. V. Shabanov, *Optics of Real Photonic Crystals: Liquid Crystal Defects and Inhomogeneities* (Siberian Branch of the Russian Academy of Sciences, Novosibirsk, 2005) [in Russian].
5. A. M. Zheltikov, Phys.—Usp. **43** (11), 1125 (2000).
6. Y. Akahane, T. Asano, B. S. Song, and S. Noda, Nature (London) **425**, 944 (2003).
7. O. Painter, R. Lee, A. Yariv, J. D. O'Brien, P. D. Dapkus, and I. Kim, Science (Washington) **284**, 1819 (1999).

8. B. M. Shi, Z. Jiang, X. F. Zhou, and X. Wang, J. Appl. Phys. **91**, 6769 (2002).

9. M. G. Martemyanov, T. V. Dolgova, and A. A. Fedyanin, JETP **98** (3), 463 (2004).

10. V. A. Belyakov and A. S. Sonin, *Optics of Cholesteric Liquid Crystals* (Nauka, Moscow, 1982).

11. Y.-C. Yang, C.-S. Kee, J.-E. Kim, and H.-Y. Park, Phys. Rev. E: Stat. Phys., Plasmas, Fluids, Relat. Interdiscip. Top. **60**, 6852 (1999).

12. V. I. Kopp and A. Z. Genack, Phys. Rev. Lett. **89**, 033901 (2003).

13. J. Schmidtke, W. Stille, H. Finkelmann, Phys. Rev. Lett. **90**, 083902 (2003).

14. A. V. Shabanov, S. Ya. Vetrov, and A. Yu. Karneev, JETP Lett. **80** (3), 181 (2004).

15. A. H. Gevorgyan and M. Z. Haratyunyan, Phys. Rev. E: Stat., Nonlinear, Soft Matter Phys. **76**, 031701 (2007).

16. V. A. Belyakov and S. V. Semenov, JETP **112** (4), 694 (2011).

17. S. Ya. Vetrov, A. Yu. Avdeeva, and I. V. Timofeev, JETP **113** (5), 755 (2011).

18. S. G. Moiseev, V. A. Ostatochnikov, and D. I. Sementsov, Kvantovaya Elektron. (Moscow) **42**, 557 (2012).

19. J. C. Maxwell Garnett, Philos. Trans. R. Soc. London, Ser. A **203**, 385 (1904).

20. A. N. Oraevskii and I. E. Protsenko, JETP Lett. **72** (9), 445 (2000).

21. L. A. Golovan, V. Yu. Timoshenko, and P. K. Kashkarov, Phys.—Usp. **50** (6), 595 (2007).

22. D. W. Berreman, J. Opt. Soc. Am. **62** (4), 502 (1972).

Translated by E.V. Chernokozhin